Preprints of the 19th World Congress
The International Federation of Automatic Control
Cape Town, South Africa. August 24-29, 2014

Control Energy Consumption and System Performance in Vector Control of Voltage Source Converters

Xiaodong Zhao *, **Kang Li** *

* *School of Electronics, Electrical Engineering and Computer Science, Queen's University Belfast, Belfast, BT9 5AH, UK (e-mail: xzhao06@qub.ac.uk, k.li@qub.ac.uk)*

Abstract: Power electronics plays an important role in the control and conversion of modern electric power systems. In particular, to integrate various renewable energies using DC transmissions and to provide more flexible power control in AC systems, significant efforts have been made in the modulation and control of power electronics devices. Pulse width modulation (PWM) is a well developed technology in the conversion between AC and DC power sources, especially for the purpose of harmonics reduction and energy optimization. As a fundamental decoupled control method, vector control with PI controllers has been widely used in power systems. However, significant power loss occurs during the operation of these devices, and the loss is often dissipated in the form of heat, leading to significant maintenance effort. Though much work has been done to improve the power electronics design, little has focused so far on the investigation of the controller design to reduce the controller energy consumption (leading to power loss in power electronics) while maintaining acceptable system performance. This paper aims to bridge the gap and investigates their correlations. It is shown a more thoughtful controller design can achieve better balance between energy consumption in power electronics control and system performance, which potentially leads to significant energy saving for integration of renewable power sources.

Keywords: VSC; renewable energy; power loss; system performance; PI controller;

1. INTRODUCTION

To meet more stringent legislations on environment protection while to offer new alternative solutions to non-renewable fossil fuel, various renewable energies are promised to be integrated to existing AC power systems, especially the integration of off-shore wind farms (Association et al. [2005]). The integration of renewable energy sources into the existing electrical grid has brought forward several technical challenges which necessitate the adoption of high voltage direct current (HVDC) transmission lines that draw little capacitive current compared with high voltage alternate current (HVAC) solutions. Voltage source converters (VSC), working as an interface between DC and AC networks, offer a number of advantages in comparison with traditional line commutated converters (LCC). For example, VSC using high voltage IGBT is capable of switching at a higher operating frequency, and VSC-HVDC can achieve independent control of active and reactive powers, fast and reversible control of power flow, and asynchronously decoupling with AC grids.

The operation and control of VSCs have been well researched in the literature. Popular approaches include model predictive control (Vargas et al. [2007]), voltage oriented vector control (Cortes et al. [2008]). Voltage oriented control (VOC), which guarantees high dynamic and static performances via an internal current control loop, has become very popular in recent years (Kaźmierkowski and Krishnan [2002]).

As a commonly used modulation technique for controlling power electronic devices, PWM is fundamental for the VSC operation, including sinusoidal pulse width modulation, space vector PWM, etc. (Moustafa [2011]). Further, a number of researches have been carried out on harmonics reduction and energy optimization in power electronics control (Holtz and Qi [2013], Wiechmann et al. [2008], Chung and Sul [1999], Kolar et al. [1991]). However, these researches mainly focus on the PWM structure design to reduce the power loss during switching operation and on vector control tuning to achieve better system dynamic performance. Although the PWM control frequency can be optimized to reduce power losses, little has been done so far on investigating the correlation between vector control parameter design and power loss reduction, and how the controller design can help to reduce the power loss in power electronics and in the meantime, maintaining desirable system performance.

It is well known that significant power loss occurs during the operation of these devices, and the loss is often dissipated in the form of heat, leading to remarkable main-

[1] This work was partially supported by UK EPSRC under grant EP/L001063/1, China NSFC under grants 61271347 and 61273040, and Shanghai Rising Star programme 12QA1401100. X Zhao would like to thank Chinese Scholarship Council (CSC) for the financial support.

Copyright © 2014 IFAC

tenance effort. Therefore it is essential to investigate the power loss and its relation to system real-time operation and control, thus guiding the proper design of the controller used in the system. This paper aims to bridge the gap and it is shown a more thoughtful controller design can achieve better balance between energy consumption in power electronics control and system control performance, which potentially leads to significant energy saving in power electronics control for integration of renewable power sources. It shows that this relation is non-linear and a better controller design can achieve a good trade-off between power loss and system performance.

This paper is organized as below. In section II, the VSC module and vector control method are outlined. Power consumption study of a VSC due to different controller designs is carried out in Section III. In Section IV, the correlation between controller energy consumption and system performance is analysed for DC voltage controller and current loop controller. In Section V, simulation results based on Matlab/Simulink are carried out to validate the proposed design method. Finally, conclusion is drawn in Section VI.

2. VSC MODEL AND VECTOR CONTROL

In this paper, a generic two level three phase converter bridge as shown in Fig. 1 is investigated. There are two

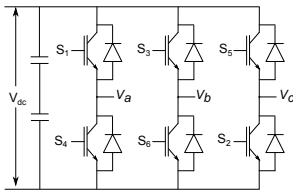

Fig. 1. Two level three phase voltage source converter

IGBTs and diodes in each phase. Every IGBT works with the opposite diode during a half AC cycle. The switching pulse signals for IGBTs are provided by a PWM modulator. Thus the main purpose of the vector controller can be treated as providing a reference for the modulator.

The basic structure of the VSC vector controller includes two feedback loops: an inner current loop supplies signals for PWM modulator to provide gate signals for IGBT, and an outer voltage loop regulates the DC voltage or active power and provides the current reference. The overall diagram of the VSC controller is shown in Figure 2.

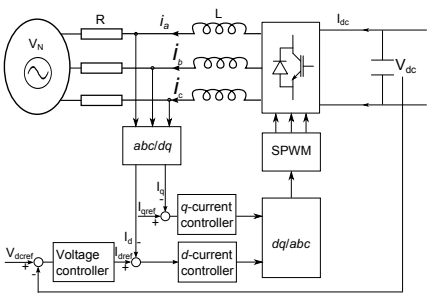

Fig. 2. Basic control scheme of VSC

In this paper, the inner current controller and the DC voltage controller are analysed and designed considering both system performance and power losses.

2.1 Inner current controller

Applying the commonly used vector conversion method, every set of three phase voltages and currents can be represented by a rotating vector respectively, using their instantaneous values. The d-axis of the rotating frame is in phase with the voltage phasor at the point of common coupling (PCC). In this way the q-axis component of the voltage becomes zero. After the abc/dq transformation, the AC side circuit equation takes the form of (1).

$$\begin{aligned} L\frac{di_d}{dt} + Ri_d &= V_{Cd} - V_{Nd} + \omega L i_q \\ L\frac{di_q}{dt} + Ri_q &= V_{Cq} - V_{Nq} - \omega L i_d \end{aligned} \tag{1}$$

The operation of VSC requires i_d and i_q to follow varying reference points. So currents of i_d and i_q can be controlled independently by acting on a set of auxiliary inputs as

$$u_d = L\frac{di_d}{dt} = k_{p1}(i_d^* - i_d) + k_{i1}\int (i_d^* - i_d)dt \tag{2}$$

where k_{p1} and k_{i1} are the proportional and integral gains of the current controller. The PI controller of d and q-axis can be set using the same parameters. The output of the PI controller compensate voltage drops on the reactor and the feed forward of AC network voltage can respond to the AC network voltage change. After decoupling, the current control loop can be simplified as shown in Figure 3. The open loop transfer function of the inner current loop can be derived as,

$$G_{open} = (K_p + \frac{K_i}{s})\frac{e^{-1/f_p s}}{sL + R} \tag{3}$$

It is clear that the close loop transfer function can be drawn as a second order system if the time delay is small enough to be omitted.

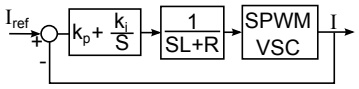

Fig. 3. Simplified inner current control loop

2.2 DC voltage controller

For a typically DC voltage regulating terminal, VSC on the DC side can be modelled as a controlled current source, as shown in Fig. 4.

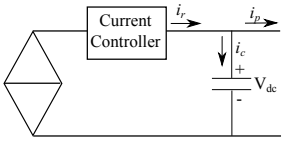

Fig. 4. VSC DC side model

A PI controller is normally used to control the DC voltage at a desired level for the DC voltage regulator. The output

of the PI controller is used as the reference signal for the inner current loop to compensate capacitor charging current. Fig. 5 shows the diagram of the voltage regulator, where V_{ref} is the reference voltage, i_p is the input from the power transmission and is considered as a disturbance.

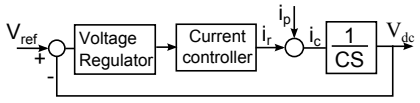

Fig. 5. DC voltage controller structure

By considering V_{ref} as input, V_{dc} as system output, the closed loop transfer function for voltage regulation can be given as

$$\frac{V_{dc}}{V_{ref}} = \frac{\frac{PI(s)}{Cs}}{1+\frac{PI(s)}{Cs}} \tag{4}$$

Considering i_p as input, i_r as output, it can be shown that the closed loop model for voltage regulation and current following are the same (Chen et al. [2012]).

3. POWER LOSS FROM A VOLTAGE SOURCE CONVERTER

For a power electronics device such as a VSC, the power losses incurred are due to the voltage drops during turned-on status and undesirable switching characteristics during switching actions. These two parts form the conduction losses and switching losses respectively, each being calculated by adding individual IGBT and diode losses in each bridge arm. Further, although often neglected in comparison with converter losses, AC side reactor and transformer losses caused by the internal resistance are related to the inner current loop and can be calculated using AC side currents.

3.1 VSC conduction loss

The forward voltage-current characteristics of a conducting IGBT and diode and can be approximated by the following linear equations:

$$\begin{aligned} V_{ft} &= V_{ft0} + i_f R_{ft} \\ V_{fd} &= V_{fd0} + i_f R_{fd} \end{aligned} \tag{5}$$

For a PWM cycle, define the relative turn-on time of one IGBT as α_t, then the relative conducting time of diode in the opposite arm is

$$\alpha_d = 1 - \alpha_t \tag{6}$$

Assuming that a simple continuous high frequency PWM modulation is used, the forwarding current of the power electronic devices can be treated as sinusoidal [Kolar et al., 1991]:

$$i_f = Icos(\theta - \phi) \tag{7}$$

where ϕ is the phase difference between phase voltage and current. The relative conduction time is

$$\alpha_t = \frac{1}{2}[1 + Mcos\theta] \tag{8}$$

where M is the modulation index.

The conduction losses can be then obtained by integration over a half AC period and taking the average,

$$\begin{aligned} P_{ft} &= \frac{1}{2\pi}\int_{-\frac{\pi}{2}+\phi}^{\frac{\pi}{2}+\phi}(V_{ft0}\alpha_t i_f + R_{ft}\alpha_t i_f^2)\mathrm{d}\theta \\ &= V_{ft0}I(\frac{1}{2\pi} + \frac{M}{8}cos\phi) + R_{ft}I^2(\frac{1}{8} + \frac{M}{3\pi}cos\phi) \end{aligned} \tag{9}$$

$$\begin{aligned} P_{fd} &= \frac{1}{2\pi}\int_{-\frac{\pi}{2}+\phi}^{\frac{\pi}{2}+\phi}(V_{fd0}\alpha_d i_f + R_{fd}\alpha_d i_f^2)\mathrm{d}\theta \\ &= V_{fd0}I(\frac{1}{2\pi} - \frac{M}{8}cos\phi) + R_{fd}I^2(\frac{1}{8} - \frac{M}{3\pi}cos\phi) \end{aligned} \tag{10}$$

Assume that each IGBT and diode has the same characteristic, which should not cause much error in most cases, then the total power consumption of a three phase converter becomes

$$P_c = 6(P_{fd} + P_{ft}) = \frac{6V_0 I}{\pi} + \frac{3R_f I^2}{2} \tag{11}$$

It is clear that the conduction loss in a VSC is mainly related to the current amplitude, which is determined by the DC voltage controller output.

3.2 Switching loss

Switching loss is caused by the rise and fall time of a IGBT during switching operations. It has been shown that the switching loss consists of turn-on, turn-off and recovery losses. A linear relation of switching loss with switched current is obtained through theoretical and experimental results in Casanellas [1994], Chung and Sul [1999], Kolar et al. [1991].

$$P_{sw} = k_{td} I f_{sw} \tag{12}$$

where k_{td} is an empirical constant from manufacturing data and f_{sw} is the switching frequency.

3.3 AC conduction loss

As mentioned in the previous part, inner current loop is used to compensate voltage drops due to the AC side inductance and resistance, including reactor and transformer. This relatively small voltage sag due to the AC resistance leads to the loss of active power which needs to be considered as well.

The AC side current is denoted as i_d and i_q after dq vector transformation, so the power loss on the resistor R can be calculated as

$$P_r = \frac{3}{2}(i_d^2 + i_q^2)R \tag{13}$$

4. CORRELATION OF POWER LOSS AND CONTROL PERFORMANCE FOR VECTOR CONTROL

4.1 PI controller synthesis - stability consideration

Current controller The output of the PI current controller is actually used to compensate the voltage drop in

the AC line resistor and inductor. The range of the PI controller parameters is limited by the PWM modulation switching frequency in the VSC. If the PWM switching frequency is f_p, then the controller acts at a time interval of $\Delta t = 1/10f_p$. The open loop transfer function of the PI current loop can be obtained using a unit time delay model of the PWM modulator:

$$G(s) = \frac{(K_p + K_i/s)e^{-1/f_p s}}{(R + Ls)} \tag{14}$$

where $1/f_p s$ is the PWM modulator time delay. Using the first order Pade approximation, the delay can be approximated by

$$e^{-1/f_p s} = \frac{-s + 2f_p}{s + 2f_p} \tag{15}$$

Thus the characteristic equation of the current loop is given as

$$\begin{aligned} C_e &= Ls^3 + (2f_pL - Kp + R)s^2 \\ &+(2f_pK_p - K_i + 2TR)s + 2TK_i \end{aligned} \tag{16}$$

Apply the Routh Criterion, the stable boundaries of the PI controller parameters K_p and K_i can be found as below,

$$\begin{aligned} &0 < K_p < 2f_pL + R \\ &0 < K_i < \frac{(2f_pL - K_p + R)(2TK_p + 2TR)}{4f_pL - K_p + R} \end{aligned} \tag{17}$$

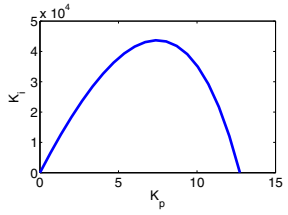

Fig. 6. Relation between K_p and K_i of current controller

The relation between acceptable K_p and K_i that make the system stable is shown in Fig. 6. This is a rather broad range for the controller. Due to frequency and time response considerations, the actual range is much smaller.

Voltage controller Similar to the current controller, the open loop transfer function of the voltage loop can be obtained using a time delay model of the inner current loop. Thus the characteristic equation of the voltage loop can be given as

$$C_e = Cs^3 + (2f_iC - K_p)s^2 + (2TK_p - K_i)s + 2TK_i \tag{18}$$

Apply the Routh Criterion again, the stable boundaries of K_p and K_i are given below and also shown in Fig. 7.

$$\begin{aligned} &0 < K_p < 2f_iC \\ &0 < K_i < \frac{2f_iK_p(2f_iC - K_p)}{4f_iC - K_p} \end{aligned} \tag{19}$$

4.2 Correlation of system performance and power loss

Based on the optimal control concept, the performance of the current controller can be assessed by its tracking error,

$$E_y = \sum (i_{cref} - i)^2 \tag{20}$$

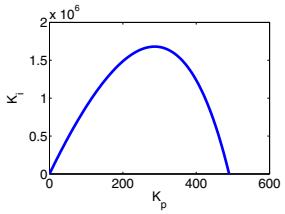

Fig. 7. Relation between K_p and K_i of voltage controller

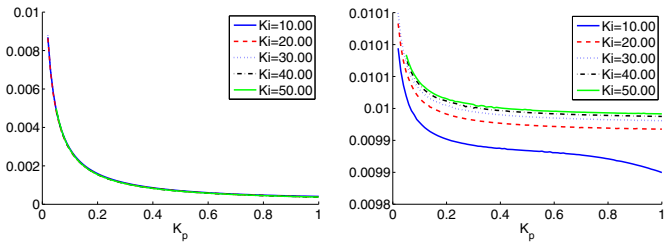

(a) performance (b) energy

Fig. 8. Current controller control energy and performance

where i_{cref} is the reference signal for the current controller, and i is the measured current feedback. Power loss for current controller is the power loss on the AC side resistance.

$$E_u = P_r \tag{21}$$

The control purpose therefore for the current controller is to reduce the power loss on AC side resistance while maintaining desirable tracking performance.

Voltage controller performance based on DC voltage fluctuation can be defined as the squared error with respect to the DC voltage reference,

$$Ey = \sum (V_{dcref} - V_{dc})^2 \tag{22}$$

The power loss for the voltage controller is related to the VSC power losses, e.g., conduction loss and switching loss.

$$E_u = \sum (P_{ft} + P_{fd} + P_{sw}) \tag{23}$$

4.3 Relation of power loss and control performance

After the feasible ranges of K_p and K_i of each controller are deduced, the system performance and power loss due to the control actions for various pairs of K_p and K_i can be studied to investigate the best trade-off between the power loss reduction and desirable system performance. To achieve this, for each controller, the two control parameters K_p and K_i are changed incrementally to inspect the effect.

Figure 8 shows the correlation of system tracking error variation as the proportional gain K_p changes for the current controller. From Fig. 8a-8b, the following observations can be drawn.

(1) For a fixed integral gain K_i, as the proportional gain K_p increases, the tracking error decrease. However the relation between the power loss and tracking performance is non-linear. After crossing a certain value of K_p, further increase of control effort (hence inducing more power loss) will have much limited effect on the improvement of the tracking performance.

(2) For the same K_p, the effect of K_i on tracking performance is very small. However, for a bigger K_i, more power loss is incurred.

For the voltage controller, the main objective of the controller is to maintain the DC voltage. System performance and power loss due to control actions in the power electronics for this problem are demonstrated in Fig. 9. It is obvious that the similar result can be drawn. Furthermore, it can be shown that there exists a minimum value of the power loss with respect to K_p.

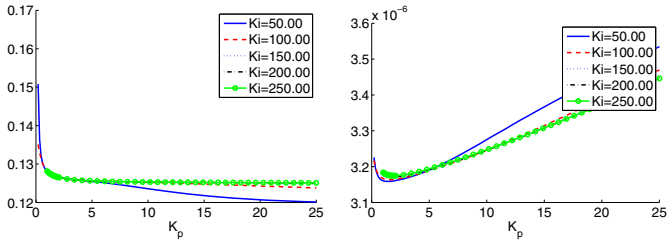

(a) performance (b) energy

Fig. 9. Voltage controller control energy and performance

The unit of control energy in Fig. 8-9 is per-unit. From Fig. 8-9, it can be concluded that through a proper design, power loss on the power electronics devices can be reduced while maintaining almost the same performance.

4.4 Sensitivity analysis

In order to further investigate the non-linear relation between power loss due to control actions and system performance, the following measurements are defined.

Change of control effort (power loss) and tracking error:

$$\begin{aligned} D_u(k) &= E_u(k) - E_u(k-1) \\ D_y(k) &= E_y(k) - E_y(k-1) \end{aligned} \tag{24}$$

Change rate of control effort (power loss) and system performance,

$$R_u(k) = \frac{D_u(k)}{E_u(k-1)}, R_y(k) = \frac{D_y(k)}{E_y(k-1)} \tag{25}$$

Sensitivity of system performance with respect to the change of control effort (power loss):

$$S_{yu}(k) = \frac{D_y(k)}{D_u(k)} \tag{26}$$

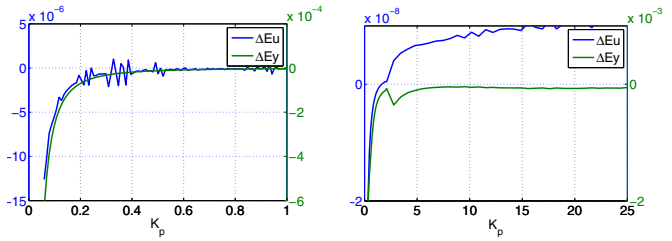

(a) Current controller $K_i = 30$ (b) Voltage controller $K_i = 100$

Fig. 10. Change of control energy and performance

Choosing a fixed K_i for both the current and voltage controllers, Fig. 10 shows the controller power loss and system performance change with respect to K_p. From Fig. 10b, it is shown that D_u reaches zero when K_p reaches a certain value, indicating that this is the point with the lowest E_u. Once K_p passes this point, the power loss will continue to increase, however tracking performance reduces very little as K_p increases.

For the current controller, due to the fact that the power loss and system performance both depends on the output current, they follow the same change pattern.

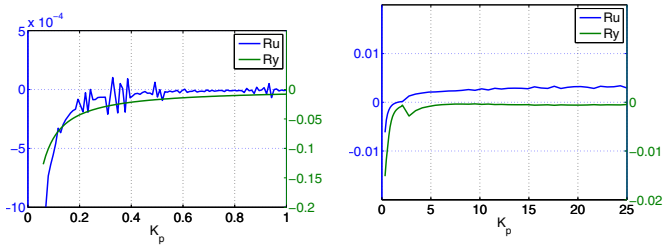

(a) Current controller $K_i = 30$ (b) Voltage controller $K_i = 100$

Fig. 11. Control energy and performance change rate

This result is also supported by the change rate analysis, as shown in Fig. 11. The change rate of the controller will reach zero for certain point of K_p. In Fig. 12, the sensitivity

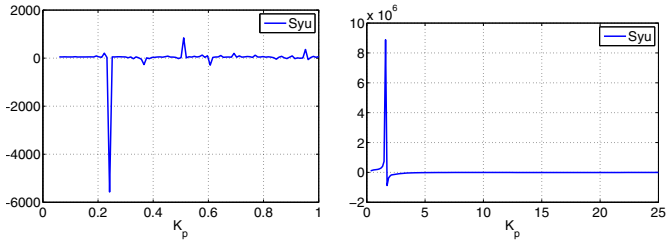

(a) Current controller $K_i = 30$ (b) Voltage controller $K_i = 100$

Fig. 12. Controller sensitivity

plot shows that further increase of control effort (hence power loss) could hardly improve the tracking performance when K_p is greater than 0.4 for the current controller and 5 for the voltage controller. This concludes that more control energy will be consumed while the system performance is not improving.

This analysis has thus shown that,

(1) Proportional gain K_p has much more effect than integral gain K_i on system performance and power loss due to control actions for the voltage controller.
(2) K_i has much more effect than K_p on system performance and control energy for the current controller.
(3) There exists a value for K_p to achieve the lowest control energy while maintaining almost the same performance, this can be used as a guidance for choosing suitable parameter settings for PI controller in power electronics control.

5. SIMULATION STUDY

To visualize the system dynamic performance of the vector controller for difference settings of K_p and K_i, simulations were carried out using Matlab Simulink toolbox

based on the VSC power loss model built before. Parameters of the simulated system are listed in Table 1. System performance and power losses are summarised in Table 2. For a time domain simulation, the related system performance and power losses are integrated based on simulation time. Thus the unit for system performance is changed to MA^2 and for power losses is MJ.

Table 1: *Simulation parameters*

Vdc	400 kV	AC voltage	240 kV
Active power	500 MW	Reactive power	0 Var
V_{f0} and V_{d0}	2V	R_{ft} and R_{dt}	$1m\Omega$
	μs	Ksw	$2 \cdot 10^{-4}$

Table 2: *Power losses for different K_p, K_i*

Current controller			Voltage controller		
Kp/Ki	Ey (MA^2)	Eu (MJ)	Kp/Ki	Ey (MV^2)	Eu (kJ))
0.5/5	1.55	5.1186	5/100	141.83	1.43
0.5/10	1.53	5.1447	10/100	100.32	1.49
0.5/20	1.52	5.1555	15/100	95.49	1.51
0.5/30	1.51	5.1591	20/100	93.66	1.52
0.5/40	1.51	5.1609	25/100	92.62	1.53

The current controller response is presented in Fig 13. The reference current raised from 0 to 1.5 kA at time t=0.3s. It can be seen that the overall tracking error can be further reduced by increasing K_i, However, the control energy (thus power loss) increases as well. By keeping almost the same performance using control pair 0.5/5 compared with 0.5/40, the power losses in the simulated time range can be reduced by $42.3kJ$.

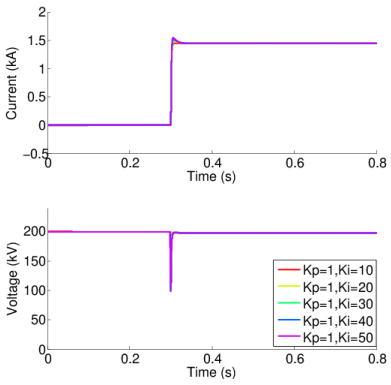

Fig. 13. Current controller dynamic response

Fig 14 shows the simulation of voltage controller. The reference voltage is decreased from 400 kV to 200 kV at t=0.3s. It can be shown that the tracking performance can be further increased, however, more power will be lost. Using control parameters 15/100, the power loss can be reduced by $0.04kJ$.

6. CONCLUSION

This paper has investigated the correlation between control energy, e.g., power loss of a VSC and vector control system performance. It has been shown that this relation is non-linear and proper controller design can achieve minimum power loss while maintaining desirable control performance. This relation can be used as a guidance for the

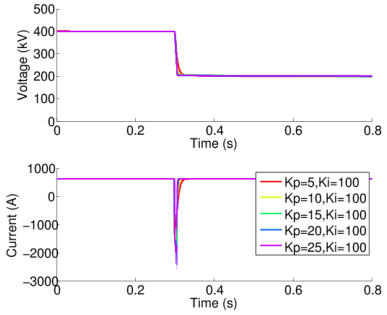

Fig. 14. Voltage controller dynamic response

parameter tuning of the PI controller in power system control. This study implicates that in the vector control and PWM modulation of VSC, if the system structure is kept unchanged, by choosing proper parameter settings for the controller, a better trade-off between system performance and control energy consumption can be reached, which potentially leads to significant energy saving in power electronics control for integration of renewable power sources.

REFERENCES

European Wind Energy Association et al. Wind force 12. *CA.[Online]. Available: http://www. ewea. org*, 2005.

F Casanellas. Losses in pwm inverters using igbts. *IEE Proceedings-Electric Power Applications*, 141(5): 235–239, 1994.

Dong Chen, Lie Xu, and Liangzhong Yao. Dc network stability and dynamic analysis using virtual impedance method. In *IECON 2012-38th Annual Conference on IEEE Industrial Electronics Society*, pages 5625–5630. IEEE, 2012.

Dae-Woong Chung and Seung-Ki Sul. Minimum-loss strategy for three-phase pwm rectifier. *Industrial Electronics, IEEE Transactions on*, 46(3):517–526, 1999.

Patricio Cortes, Marian P Kazmierkowski, Ralph M Kennel, Daniel E Quevedo, and José Rodríguez. Predictive control in power electronics and drives. *Industrial Electronics, IEEE Transactions on*, 55(12):4312–4324, 2008.

J. Holtz and Xin Qi. Optimal control of medium-voltage drives–an overview. *Industrial Electronics, IEEE Transactions on*, 60(12):5472–5481, Dec 2013.

Marian P Kaźmierkowski and Ramu Krishnan. *Control in power electronics: selected problems*. Academic press, 2002.

Johann W Kolar, Hans Ertl, and Franz C Zach. Influence of the modulation method on the conduction and switching losses of a pwm converter system. *Industry Applications, IEEE Transactions on*, 27(6):1063–1075, 1991.

M.M.Z. Moustafa. *Operating limits and dynamic average-value modelling of VSC-HVDC systems*. PhD thesis, University of Manitoba, 2011.

René Vargas, Patricio Cortés, Ulrich Ammann, and Rodríguez. Predictive control of a three-phase neutral-point-clamped inverter. *Industrial Electronics, IEEE Transactions on*, 54(5):2697–2705, 2007.

Eduardo P Wiechmann, Pablo Aqueveque, and Rolando Burgos. On the efficiency of voltage source and current source inverters for high-power drives. *Industrial Electronics, IEEE Transactions on*, 55(4):1771–1782, 2008.